water

MDPI

Article

Geochronological and Sedimentological Study of the Fluvio-Lacustrine Deposits from Shigu to Longjie: Implications for the Evolution of the Lower Jinsha River since the Early Pleistocene

Fenliang Liu [1,*], Hongshan Gao [2], Zongmeng Li [3], Changjun Huang [1], Zhen Xi [1] and Yun Xue [1]

1 School of Municipal and Geomatics Engineering, Hunan City University, Yiyang 413000, China
2 Key Laboratory of Western China's Environmental Systems (Ministry of Education), College of Earth and Environmental Sciences, Lanzhou University, Lanzhou 730000, China; gaohsh@lzu.edu.cn
3 School of Geographic Sciences, Xinyang Normal University, Xinyang 464000, China
* Correspondence: fenliangliu@126.com

Abstract: The formation of the Jinsha River drainage is a significant subject of concern in the geological and geomorphological fields. Among them, one key question is whether there was a regional paleo lake into which Lower Jinsha River drainage drained during the late Pliocene to early Pleistocene, due to massive fluvio-lacustrine sediments widely distributed in the Lower Jinsha River. Nevertheless, there has yet to be a consensus on the genesis of those fluvio-lacustrine sediments due to poor sedimentological and chronological data. In this study, to unravel the origin of those fluvio-lacustrine sediments and the formation model of the Lower Jinsha River, sedimentary characteristics, including spatial distribution, lithological composition, and stratigraphic contact relationship of those fluvio-lacustrine sediments were analyzed, and chronological determination of the fluvio-lacustrine sediments using Electron Spin Resonance and Optically stimulated luminescence method was conducted. The results show that in the Lower Jinsha River, the lacustrine sediments are mainly composed of silt and clay, with apparent horizontal bedding, stacked with fluvial cobble-gravel and sand, and are in unconformable contact with the underlying bedrock strata or paleo soil. The lacustrine sediments are spatially discontinuous and mainly distributed in the Shigu, Taoyuan, Panzhihua, and Longjie reaches. Downstream of these reaches are deeply incised gorges with an average slope >30°, and many landslide landforms and deposits can be identified here. In each reach, the lacustrine sediments were closely distributed along the trunk and tributary channels in the plane and were distributed at different altitudes, forming a sequence of lacustrine terraces. Chronological analysis shows that in different reaches, the deposition ages of lacustrine sediments are significantly different. In each reach, the deposition age of the lacustrine terraces of high altitude is older than that of low altitude. The above characteristics collectively indicate that the lacustrine sediments in the Lower Jinsha River were locally deposited by individual dammed lakes, probably induced by landslide rather than a regional paleo lake by tectonic activities. During the incision process of the river valley, landslides continuously block the river channel, forming dammed lakes, and then deposited lacustrine sediments at different elevations, forming lacustrine terraces. The lacustrine sediment of the topmost lacustrine terrace in Panzhihua reach was dated to be 1.78 Ma, combined with previous studies on the fluvial terraces, indicating the Lower Jinsha River existed and started to incise its valley before the early Pleistocene. The widespread dammed lake sediment indicates that the formation of the Jinsha River valley follows the pattern of "incision-landslide-damming-aggradation-incision".

Keywords: lacustrine sediment; terrace; river evolution; Jinsha River

Citation: Liu, F.; Gao, H.; Li, Z.; Huang, C.; Xi, Z.; Xue, Y. Geochronological and Sedimentological Study of the Fluvio-Lacustrine Deposits from Shigu to Longjie: Implications for the Evolution of the Lower Jinsha River since the Early Pleistocene. *Water* **2023**, *15*, 3613. https://doi.org/10.3390/w15203613

Academic Editor: Bommanna Krishnappan

Received: 23 August 2023
Revised: 28 September 2023
Accepted: 10 October 2023
Published: 16 October 2023

1. Introduction

The formation and evolution of great rivers is a major scientific issue concerning geomorphology [1]. The Jinsha River, the upper reaches of the Yangtze River, is an essential part of the drainage system of the southeast Tibetan Plateau. Its formation and evolution have been the primary issues concerning geologists and geomorphologists since the beginning of the 20th century because of its peculiar drainage patterns and its significance in deciphering the history of tectonic uplift [2–10].

In the past twenty years, with the development of chronology and source tracing technology, there have been more and more research results and controversies on this issue. However, they mainly focus on the following three aspects. The first aspect is the incision time of the modern Jinsha River. Many scholars have studied the incision time of the Jinsha River from different perspectives and based on various methods, but, at present, there are significant differences in the research results, which range from the late Eocene to early Pleistocene [11–20].

The second aspect is whether the Jinsha River once flowed southward. Most researchers suggest that the Jinsha River was once a tributary of the south-flowing "paleo Red River" in the southeastern Tibetan Plateau and eventually flowed to the east by river capture before Miocene [13,21,22], while some scholars hold the view that there is no connection between the paleo Jinsha River and paleo Red River [23–25].

The third aspect is whether there was a regional paleo lake into which the Lower Jinsha River drainage drained during the late Pliocene to early Pleistocene due to massive fluvio-lacustrine sediments widely distributed in the Lower Jinsha River. However, poor chronology data and sedimentary analysis of the fluvio-lacustrine sediments led to various models on the genesis of the fluvio-lacustrine sediments being proposed. One model thought that the fluvio-lacustrine sediments were deposited by tectonic-related regional paleo-lake "Xigeda" during Plio-Pleistocene, formed by damming the originally south-flowing Jinsha River [26] or east-flowing Jinsha River [27,28] due to tectonic activities, based on the similar sedimentary characteristics and deposited ages. In this model, the modern Jinsha River flowed eastward and incised down from the lacustrine sediments after the paleo lake breached at about 1.3 Ma. Another model thought that the fluvio-lacustrine sediments were deposited by individual dammed lakes induced by landslide, debris, and glaciation in the Pleistocene, and that no regional paleo lake existed [29–32].

Fluvio-lacustrine sediments preserve the past geologic and climatic records [33], as well as information about the drainage evolution [20,34]. In this paper, to unravel the genesis of the fluvio-lacustrine sediments and the formation time and pattern of the Jinsha River valley in the Lower Jinsha River, field surveys from Shigu to Longjie were conducted to measure the spatial distribution and sedimentary characteristics of the fluvio-lacustrine sediments and relative landforms. To determine the depositional model of the fluvio-lacustrine sediments and formation time of the Jinsha River valley, Electron Spin Resonance (ESR) and Optically stimulated luminescence (OSL) techniques, which were commonly used to date the burial age of the Pleistocene sediments in the lacustrine and fluvial settings, were employed to date the deposition ages of the fluvio-lacustrine sediments.

2. Geological and Geomorphic Setting

The study area is located between 99°30′ E–103°30′ N and 25°30′ N–28°00′ N (Figure 1) and belongs to the southeastern Tibetan Plateau, where the landscape is characterized by well-preserved low-relief surfaces or planation surfaces distributed between the deeply incised valleys of the Jinsha River and its tributaries [35,36].

Tectonically, the study area is located in the southeastern part of the Chuandian rhombic block, which is bounded by the sinistral Xianshuihe-Xiaojiag fault system to the northeast and the central Jinshajiang-Red River fault system to the southwest. The Chuandian rhombic block is divided into two parts by the NE-SW-trending Yalong thrust fault system, which was once part of the Longmen thrust fault during the Mesozoic [37,38]. The north part is the Songpan-Ganze terrane, which is mainly composed of strongly folded and faulted Triassic flysch and volcanoclastic rocks. The south part is the South China blocks, which consists mostly of less deformed Palaeozoic sedimentary rocks [39]. Overall, the region lacks Tertiary strata. This region has experienced a complex and protracted deformation history during the Mesozoic and Cenozoic [40]. Late Cenozoic to modern deformation across the southeastern Tibetan Plateau is mainly focused along these large strike-slip faults. The neotectonic activities are intense, and earthquakes are frequent.

The Jinsha River, originating from the Tibetan Plateau, flows first south parallel with the Mekong and Salween Rivers in the Hengduan Mountains, then makes a dramatic turn to northeast at Shigu. After that, it flows through the Yunnan Plateau, deeply incised into gorges in response to the tectonic uplift during the late Cenozoic, and makes several dramatic turns at Sanjiangkou, Taoyuan, Panzhihua, Longjie, and Xinshizhen. Finally, it flows east to enter the middle reach of the Yangtze River at Yibin, forming a strange W-shaped course. Those sharp turns may be related to river captures or conjugate faults. Terrain analysis, based on Shuttle Radar Topography Mission data, show that the valley is deeply incised, with a relief of about 2–3 km from between the plateau surface to the valley bottom, and that relatively broad valleys existed (Figure 2). The broad valley reaches from Qizong to Shigu, Zhongjiangjie to Taoyuan, Guanyinyan to Panzhihua, Longjie, and Menggu to Qiaojia. In these reaches, the valley bottom width exceeds 1 km, the channel gradient is less than 2‰, and the average valley slope is less than 30°. In addition, massive Pliocene to Pleistocene sediments are distributed here (Figure 1). Compared to the wide valley reaches, the gorge reaches are characterized by relatively narrow valley bottoms, steep channel profiles, and steep valley slopes. In the gorge reaches, paleo landslide and debris landform and depositions are common. This catastrophic process plays a vital role in shaping river valley landforms [41,42]. The dammed lake formed by landslides or debris can cause river aggradation of the upstream channel, hinder the river incision and headward erosion, and the extreme flood formed after the dammed lake breaks can cause intense erosion of the downstream river channel.

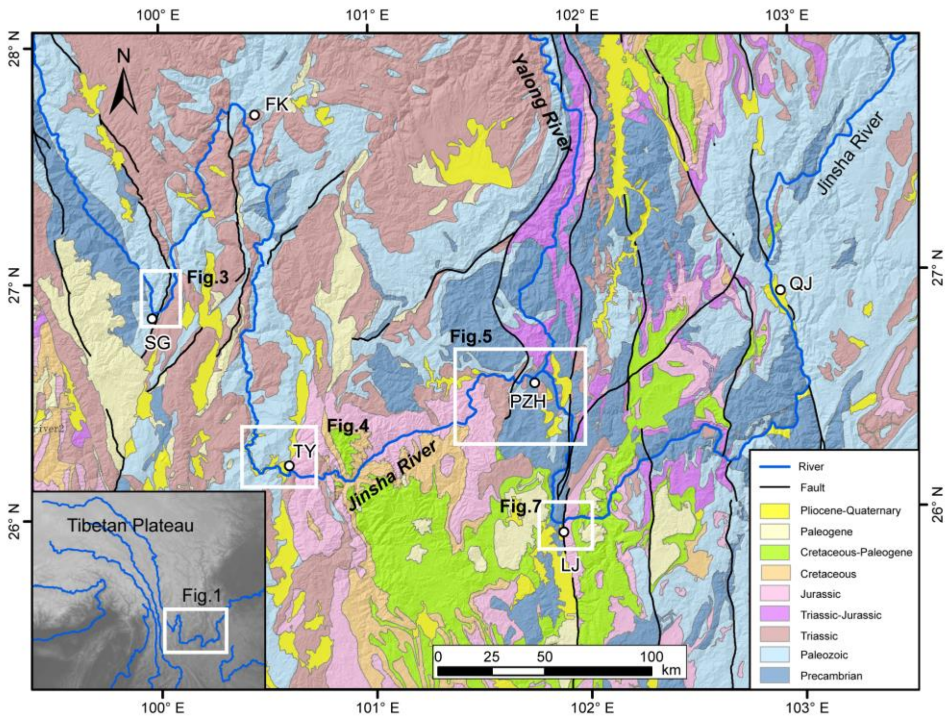

Figure 1. Simplified geological map with main rivers of the study area derived from the China 1:2,500,000 digital geological map. The inset map shows the location of Figure 1. SG: Shigu, FK: Fengke, TY: Taoyuan, PZH: Panzhihua, LJ: Longjie, QJ: Qiaojia.

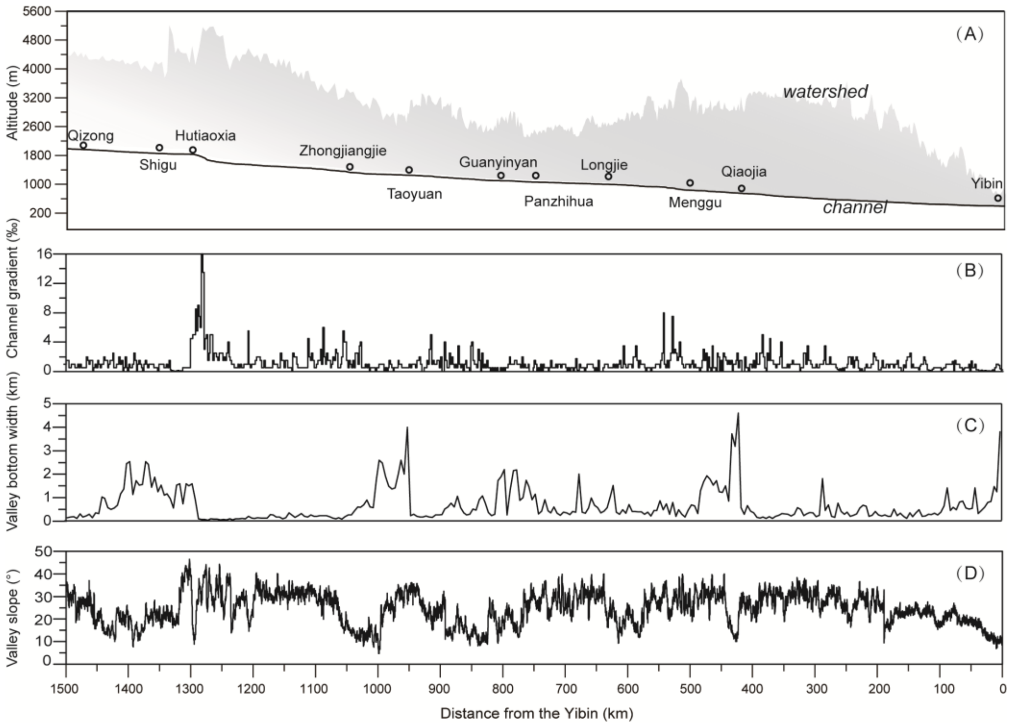

Figure 2. Morphology of the Jinsha River valley from the Qizong to Yibin. (**A**) River longitudinal profile and relief distribution along the Jinsha River. (**B**) Channel slope of the Jinsha River. (**C**) Valley bottom width of the Jinsha River. (**D**) Average valley slope along the Jinsha River.

3. Samples and Methods

3.1. Field Work

In the Jinsha River valley, fluvio-lacustrine deposits and landforms are widely developed. In this study, we chose reaches from Shigu to Longjie for investigation. Sedimentary characteristics and valley landforms, including river terraces and landslide, were described in detail in the field. The sedimentary strata's thickness and the fluvial gravel's size were measured by measuring ruler. The thickness of the fluvial gravel layer was measured from the top layer to bottom layer, and the size of fluvial gravel was obtained by measuring the average of its major and minor axes. A handheld high-resolution global positioning system directly measured the latitude, longitude, and altitude of the sampling location and the height of the terrace surface.

3.2. Dating Method

The geochronological framework for fluvio-lacustrine sediments and relative landforms is crucial regarding the river incision and aggradation process and the evolution history of the Jinsha River. In this study, we selected Electron Spin Resonance (ESR) and Optically Stimulated Luminescence (OSL) as our dating methods to measure the deposition time of the fluvio-lacustrine sediments [43–46]. These two methods have been commonly used to date the Pleistocene sediments in the lacustrine and fluvial settings because they both directly date the quartz grains of which such sediments are often composed and measure the depositional age at which quartz was buried in Quaternary sediments after the last exposure. The ESR and OSL have an age range of up to around 2.5 Ma and 200 ka, respectively. So, we use ESR to date the older sediments and OSL to date younger sediments. ESR samples were collected from the sand layer or the fluvial gravel layer that contains sand. OSL samples were collected from the sand or silt layers in the lacustrine sediments.

For ESR dating, 30 cm surface material was first scraped out at the sampling sites in order to make a fresh exposed surface. Then samples were collected from this fresh surface, ensuring shielding from direct sunlight because, when samples were exposed to sunlight or mixed with materials that were deposited later, the dating age will be underestimated. In the laboratory, the samples were partitioned into two aliquots. The first aliquot was subjected to dehydration at a controlled temperature of 50 °C for the purpose of quantifying its water content. Subsequently, this dehydrated portion was finely pulverized to yield silts with particle sizes smaller than 0.074 mm. The silt particles were then subjected to rigorous analysis at the Beijing Research Institute of Uranium Geology to determine the concentrations of uranium (U), thorium (Th), and potassium (K) using laser fluorescence, colorimetric spectrophotometry, and atomic absorption techniques, respectively. The second aliquot was sieved with water to extract grains with diameters between 100 and 140 μm. Sieved grains were soaked in H_2O_2 for 48 h to remove organic material, then soaked in 6 M HCl for 48 h to remove carbonate and disperse the grains. After soaking, the sample was etched in HF for 6 h, and then purified with water and dried under 40 °C. After magnetic separation, quartz grains were divided into 10 subsamples (about 300 mg each). The aliquots received additional gamma doses ranging from 0 to 6000 Gy using a ^{60}Co source. The quartz E′ and Ge center ESR signal intensity was measured by EMX Bruker X-band spectrometer at room temperature, with the following specifications: X-band, microwave power 0.2 or 2.0 mW for E′ and 2.0 mW for Ge, modulation amplitude 0.1 mT. The samples were measured three times in different directions to obtain the average intensity. The equivalent dose (DE) values and their errors were determined from the dose-response data, fitted with a single saturating exponential (SSE) function using the protocol and the software described by Yokoyama et al. (1985) [47] if the data show exponential change or fitted with a linear equation if the data show linear change. The dose determination was completed in the State Key Laboratory of Earthquake Dynamics, Institute of Geology, China Earthquake Administration. The contributions of α-radiation were neglected because most of the outer layers of the quartz grain had been removed by HF. The error of the ESR age is mainly obtained through estimation methods, and is generally below 15%, mainly from errors in total dose and environmental dose measurement.

Samples for OSL dating were collected from field profiles using 35 cm steel tubes after thorough cleaning. In the laboratory, the samples underwent a series of treatments to eliminate carbonate and organic matter. Specifically, 10% HCl and 30% H_2O_2 were applied to remove carbonate and organic matter, respectively [48]. Medium or coarse-grained fractions (ranging from 38–63 μm or 90–150 μm) were obtained through sieving. The medium-grained fractions underwent a two-week etching process with 35% H_2SiF_6 to remove feldspars. For the coarse-grained fractions, heavy liquids were used to separate quartz, followed by etching with 40% HF for 1 h. Fluorites were eliminated by rinsing the samples with HCl. Finally, the purity of the separates was verified using infrared diodes.

The OSL measurements were conducted at the Luminescence Dating Laboratory of the Qinghai Institute of Salt Lakes. An automated Risø TL/OSL-DA-20 reader, which was produced at the Risø Laboratory (Roskilde, Denmark), was used for OSL signal measurements. As the measurement system is highly sensitive and includes a reference radiation source, it is widely used for determining radiation doses in natural and artificial materials with applications in geological and archaeological dating. DE determination in this study was carried out using both the Single Aliquot Regenerative (SAR) protocol [49] and the Standard Growth Curve (SGC) method [48,50]). Optical measurements were conducted after applying a heating step at 260 °C for 10 s for natural and regenerative doses, and a preheating step at 220 °C for 10 s for test doses [48]. The concentrations of uranium (U), thorium (Th), and potassium (K) in each sample were determined through neutron activation analysis (NAA). The environmental dose rate was assessed by applying the conversion relation established by Aitken (1985) [51] between the elemental concentrations (U, Th, and K) and the dose rates corresponding to different minerals. To account for variations in sample composition, the efficiency of the total dose rate was adjusted considering the density of quartz and the paleowater content specific to each sample. The water content was derived by calculating the ratio of the weight of water to the weight of the dried sample. The accuracy of OSL dating is 5–10%.

4. Results

4.1. Spatial Distribution and Sedimentary Characteristics of the Fluvio-Lacustrine Sediments

In the Jinsha River valley, fluvio-lacustrine sediments are widely distributed, mainly on the relatively flat valley slopes on both sides of the trunk and tributaries of the Jinsha River, overlying on the bedrock, ancient soil, weathered crust, river alluvial, or alluvial deposits. The fluvio-lacustrine sediments are mainly comprised of gray, grayish blue, grayish yellow, and brownish yellow silt and clay, locally mixed sand and gravel, and well-developed horizontal bedding or laminae. Unlike the scattered and narrow river terraces in the river valley, the top surface of lacustrine deposits is flat and wide, gently tilting towards the river and extending upstream and downstream for a certain distance, forming a stepped terrain in the valley. In order to distinguish these terraces from the river terraces, they are referred to as lacustrine terraces in this article. Unlike the river terrace, which is is formed by fluvial incision and aggradation, the lacustrine terrace here is formed by lake depositing processes, and the terrace surface represents the paleo-lake bottom. They form a stepped terrain in the valley with river terraces, alluvial fans, and other landforms. Although the spatial distribution of lacustrine sediments is vast, the distribution along the river is not continuous, manifested as a beaded distribution. Among them, in the lower reaches of the Jinsha River, these lacustrine sediments are mainly distributed in the Shigu reach, Taoyuan reach, Panzhihua reach, Longjie reach, and Qiaojia reach. Of course, small amounts of lacustrine deposits are scattered between these reaches. Based on our investigation results of the Shigu reach, Taoyuan reach, and Panzhihua reach, combined with previous research results, we will describe the spatial distribution and sedimentary characteristics of lacustrine sedimentation and lacustrine terraces below.

4.1.1. Shigu Reach

In the Shigu reach, lacustrine sediment is mainly composed of gray, grayish blue, grayish yellow, and brownish yellow silt and clay, with locally mixed sand and gravel, and well-developed horizontal bedding or laminae (Figure 3). This set of lacustrine sediments can be traced upstream from Hutiao to Qizong. On the eastern valley profile of the Jinsha River near Qiping, one lacustrine terrace developed, with an extensive terrace surface that gently slopes towards the river. The altitude of the terrace surface is between 1870–1840 m. On the western profile, four fluvial terraces were reported to have developed on the lacustrine sediments. The height of those fluvial terraces were 43 m (T4), 25 m (T3), 20 m (T2), and 10 m (T1) above the modern riverbed, respectively [52]. In the Tiger Leaping Gorge immediately downstream of the Hutiaoxiao Vallege, the valley slope is in excess of 60°, and several colossal landslides characterized by round chair terrain can be identified. As such, the lacustrine sediments in this reach may have been deposited by a landslide-dammed lake. When the lake breached, the river incised the lacustrine sediments, forming four river terraces on it. In addition, nearby at Qizong, the upstream terminal of lacustrine sediments distribution, a set of fluvial gravel layers of a thickness of about 10 m was deposited on the valley (photo b in Figure 3), implying an intense aggradation event here. This aggradation event was possibly caused by the base level rising due to dammed lake formation.

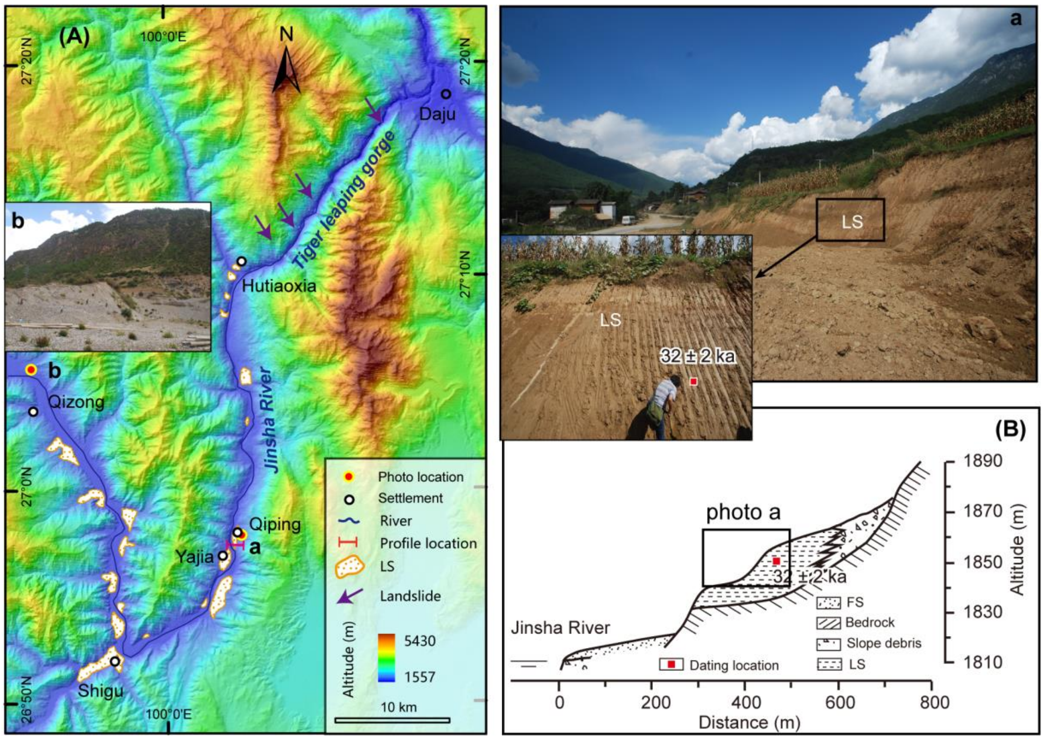

Figure 3. Lacustrine sediment and field photos in Shigu reach of the Jinsha River. (**A**) spatial distribution of the lacustrine sediment. (**B**) lacustrine sediment and lacustrine terrace at Qiping. LS: Lacustrine sediment; FS: Fluvial sand.

4.1.2. Taoyuan Reach

In the Taoyuan reach, the lacustrine sediments are mainly composed of light yellow, grayish-yellow silt, and silty clay. Due to the infiltration of red paleo-soil and weathered crust, some areas appear reddish brown (photo a in Figure 4). The horizontal bedding of lacustrine sediment is developed, and the surface of lacustrine terraces is slightly inclined towards the river. Near Liujia Village on the west bank of the Jinsha River, the exposed profile shows that this set of lacustrine sediment directly overlies the fluvial gravels, and there is a set of fluvial sand and gravel lenses mixed in the lacustrine sediment (photo b in Figure 4). The fluvial gravel is well-rounded and has particle size of 5–10 cm. The lacustrine sediments can be traced continuously from Zhaizicun downstream to Zhongjiangjie upstream, with a length of about 46 km along the river. The lacustrine sediments are distributed along the trunk and tributary valleys of the Jinsha River and presents a dendritic shape on the plane (Figure 4A). The lacustrine sediments are distributed at an altitude of 1500–1180 m, forming a broad terrace landform on both sides of the channel. On the north bank of the river near Taoyuan, three lacustrine terraces developed (Figure 4B), with a tread height of 150–120 m (T3), 90–70 m (T2), and 20 m (T1) above river level, respectively. The lacustrine sediment of T2 and T1 all overlap on the fluvial gravel layer (photo c in Figure 4). At Zhaizicun, immediately downstream of the lacustrine sediments, huge damming landslides can be identified [53]. As such, we infer that lacustrine sediments in the Taoyuan reach were deposited by a dammed lake induced by landslides at Zhaizicun. Three lacustrine terraces imply that there are three river damming events in different epochs.

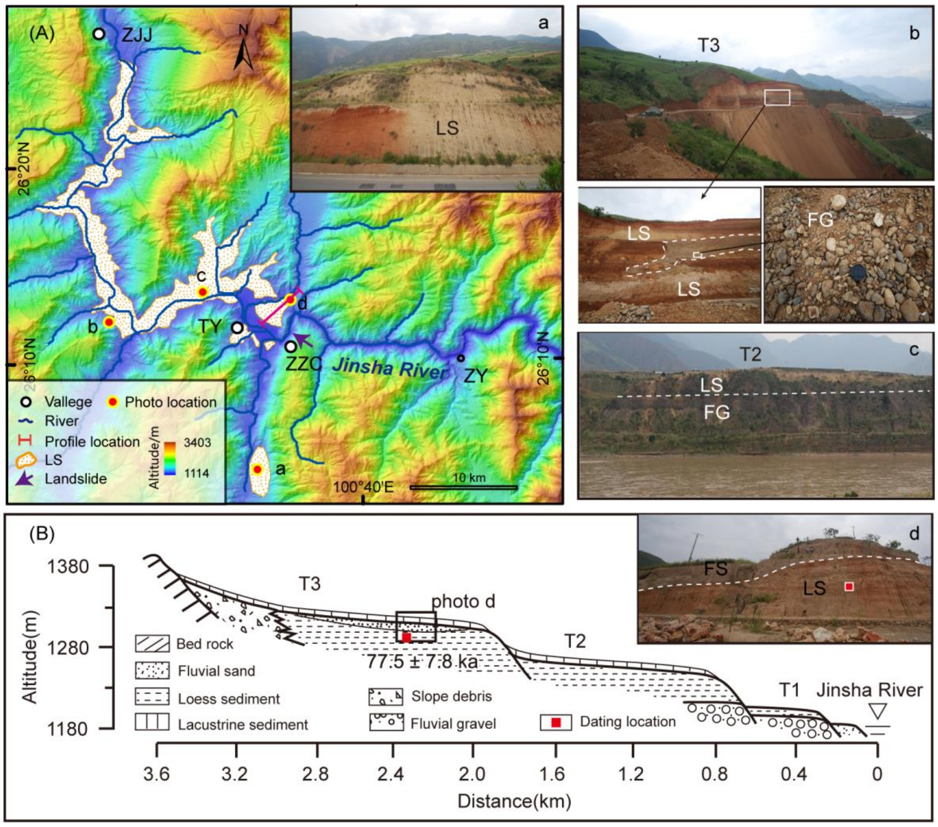

Figure 4. Lacustrine sediment and field photos in Taoyuan reach of the Jinsha River. (**A**) spatial distribution of lacustrine sediment. (**B**) lacustrine sediment profile and lacustrine terraces at Taoyuan. ZJJ: Zhongjiangjie, TY: Taoyuan; ZZC: Zhaizicun; ZY: Zhongying; LS: Lacustrine sediment; FG: Fluvial gravel, FS: Fluvial sand.

4.1.3. Panzhihua Reach

In the Panzhihua reach, lacustrine sediments are mainly composed of light yellow and gray clay, silt, and fine sand, with apparent horizontal bedding. In terms of spatial distribution, this set of lacustrine deposits can be traced upstream from Lazha to Guanyinyan, mainly developing along the valleys of the trunk and tributaries of the Jinsha River (Figure 5). For example, lacustrine sediments are very developed in the tributary basins of the Tangba River, Dahe River, Bara River, and Yanyang River. Overall, the distribution of lacustrine sediments is closely related to the river channels, exhibiting a dendritic distribution pattern on the plane. Lacustrine sediments are distributed below an altitude of 1600 m, forming staircase terraces in the valley.

Near Guanyinyan, three terraces composed of lacustrine deposits can be seen on the west bank of the Jinsha River (Figure 6), with tread heights of 121 m (T3), 114 m (T2), and 17 m (T1) above riverbed level, respectively. Among them, the surface of T3 and T2 are extensive, reaching tens of meters. The terrace surface gently tilts towards the river, and a set of fluvial gravels overlay on the lacustrine deposits (Figure 6). The gravel has good roundness and complex lithology, with a particle size of 5–30 cm and a thickness of 2–3 m. No fluvial gravel was found on T1. In the tributary Tangba River basin, lacustrine deposits occur everywhere. At the Wanzitou, a lacustrine terrace can be seen. The height of this terrace tread is about 182 m above the riverbed level of the Jinsha River. On this terrace, fluvial gravels overlay on the lacustrine deposits. At the Jingtang, not far downstream of Guanyinyan, a set of grayish yellow lacustrine sediments can be seen directly overlying on the fluvial gravels; the top surface of the lacustrine sediment is about 308 m above the modern riverbed (photo b in Figure 5).

On the river valley near Bingcaogang, lacustrine sediments are continuously distributed on the profile, forming seven lacustrine terraces (Figure 6). The surface heights of those terraces are about 470 m (T7), 430 m (T6), 360 m (T5), 300 m (T4), 250 m (T3), 220 m (T2), and 180 m (T1), respectively. The study by Zhao et al. (2008) [54] showed that the lacustrine sediments in the area were covered with fluvial gravels. However, we did not see these fluvial gravels during field investigations, which may have been damaged by later urban construction. Despite this, a set of fluvial gravels underlies the lacustrine sediments of T1. The exposed thickness of this set of fluvial gravels is about 3 m, with good roundness and a particle size of about 5–30 cm.

In the tributaries of the Bara River and Yanyang River basins, lacustrine sediments are widely distributed. On multiple outcrop profiles, lacustrine sediments can be seen overlying fluvial gravels, red weathered crust, ancient soil, or granite bedrock. Among them, on the river valley profile near Sanduizi, five lacustrine terraces developed, with surface heights of about 530 m (T5), 400 m (T4), 350 m (T3), 240 m (T2), and 170 m (T1) above the modern riverbed, respectively. Lacustrine sediment of T5 directly overlays the granite bedrock. A layer of fluvial gravel is sandwiched in the lacustrine sediment of T1, with a thickness of about 2–3 m, good roundness, and complex lithology (Figure 6). On the valley profile at Lazha, three lacustrine terraces developed (Figure 6). The heights of those terraces are 730 m (T3), 500 m (T2), and 175 m (T1) above riverbed level, respectively.

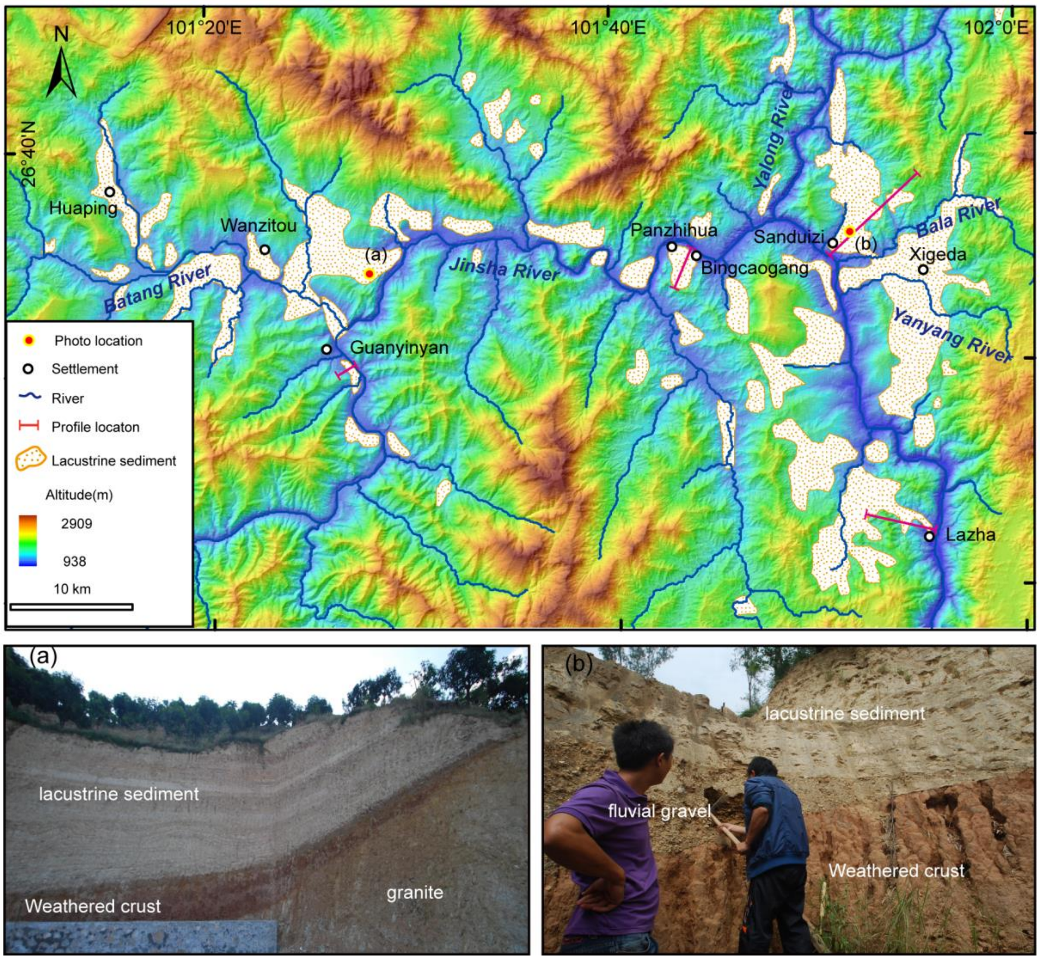

Figure 5. Spatial distribution and field photos of the Lacustrine sediment in Panzhihua reach of the Jinsha River. Red lines show the profile locations of the Figure 6.

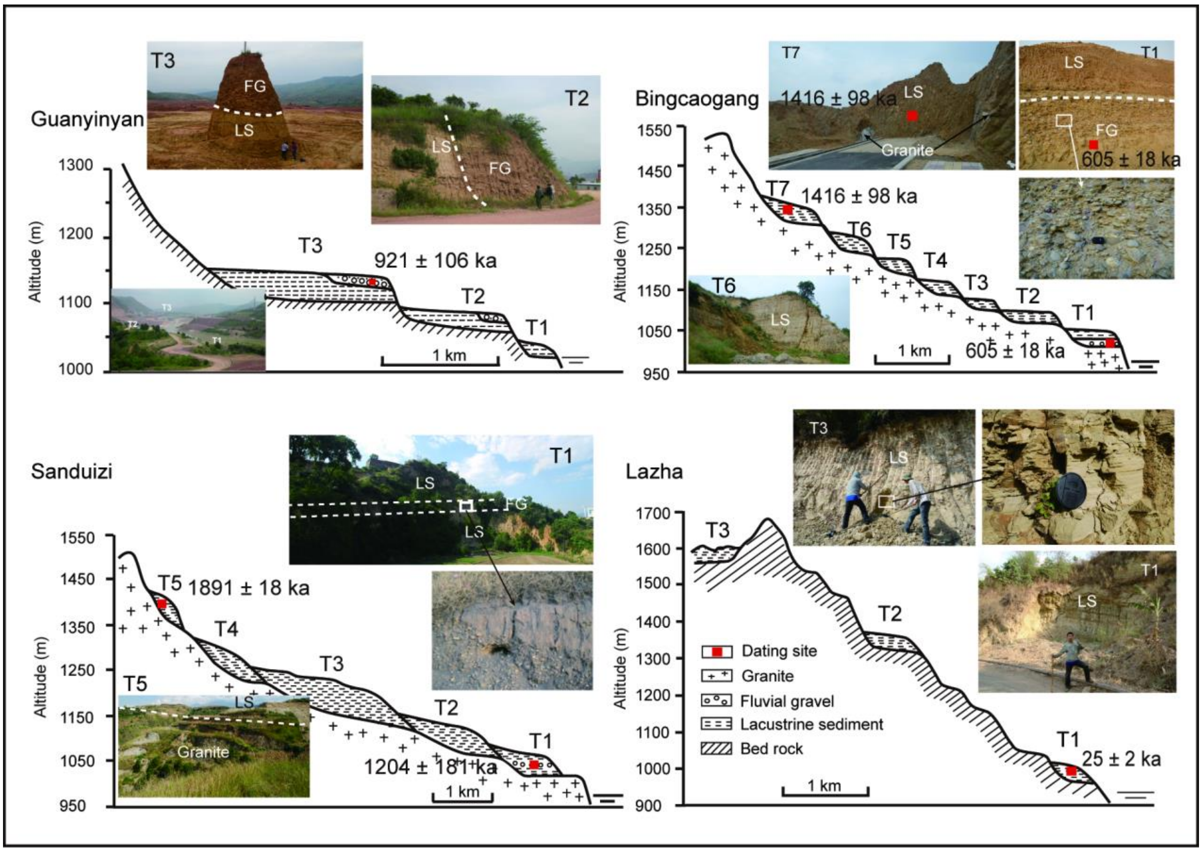

Figure 6. Profiles and photos showing the lacustrine sediments and lacustrine terraces at Guanyinyan, Bingcaogang, Sanduizi, and Lazha of the Jinsha River, respectively.

Many ancient and modern landslide landforms can be seen downstream of this reach. As such, we inferred that the lacustrine sediments were landslide dammed lake sediments. The sedimentary characteristics of the lacustrine deposits in this reach suggest that the Jinsha River was dammed at least seven times with the valley incision in the geologic history. When these ancient dammed lakes breached, the river incised down from the lacustrine sediments, forming river terraces.

4.1.4. Longjie Reach

In the Longjie reach, lacustrine sediment is mainly composed of grayish black, grayish white, grayish-yellow silt, and clay, with obvious horizontal bedding. This set of lacustrine sediment is mainly distributed in the Longjie Basin and is generally exposed on both sides of the Longchuan River north of Yuxian (Figure 7A). The lacustrine sediment unconformity overlies the red Yuanmou Formation strata (Figure 7B). Four river terraces are developed on the lacustrine sediment at the intersection of the Longchuan River and Jinsha River (Figure 7C). In the downstream reach, the valley slope is in excess of 30°, and several huge landslides characterized by round chair terrain can be identified; these include the Baimakou landslide, which was reported to have dammed the Jinsha River. As such, we think that the lacustrine sediments in this reach may have been deposited by a landslide dammed lake. When the lake breached, the river incised the lacustrine sediments, forming four river terraces on it.

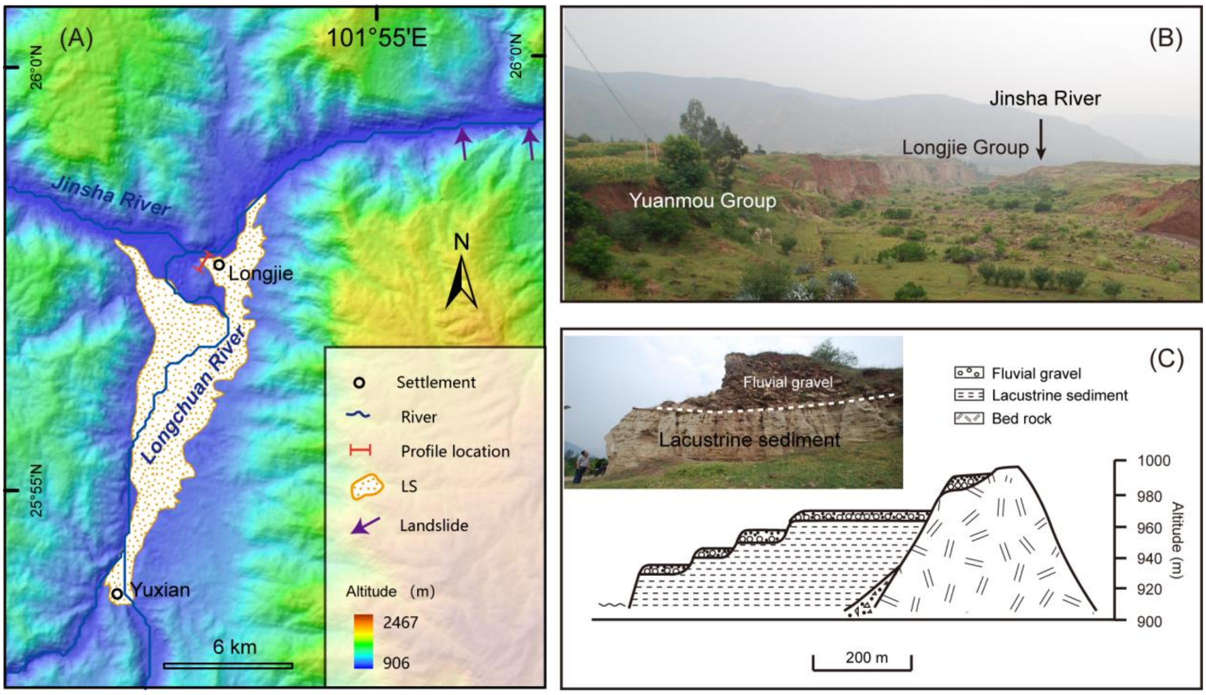

Figure 7. Lacustrine sediment and field photos in Longjie reach of the Jinsha River. (**A**) Spatial distribution of the lacustrine sediment, red line showing the profile location in Figure 7C. (**B**) The relationship of the lacustrine sediment (Longjie Group) and the Yuanmou Group. (**C**) Profiles and photos showing the lacustrine sediments and lacustrine terraces at Longjie.

4.2. Dating Results

Due to the fine grain size of lacustrine sediments, we did not extract enough quartz grains between 100 and 140 µm for ESR dating in many samples; as such, we only received six reliable ESR ages. The ESR signal spectrum of typical samples shows clear E 'centers (g = 2.001) and Ge centers (g = 1.9770) (Figure 8A). The additional irradiation dose response curve shows an exponential increase in the response of signal intensity to dose, and the curve is well fitted with a goodness of fit parameter (R^2) greater than 0.98 (Figure 8B). By using an exponential equation to fit and extrapolate until the ESR signal strength is zero, the Paleodose (AD) of the sample can be calculated. The measured AD of the samples are between 1188–6035 Gy (Table 1), and the AD of most samples are less than the maximum irradiation dose of 6000 Gy, meeting the irradiation dose requirements for ESR dating. The annual dose (d) was calculated based on the content of U, Th, and K using Bell's formula. Due to the surface of quartz particles having already been eroded when removing feldspar, the contribution of α radiation can be ignored. Then, d was adjusted by the water content. Finally, the ESR age (t) of the samples were calculated using the formula t = AD/d. Considering all parameters, the total error of the ESR ages was estimate to less than 15%. There are many influencing factors for ESR dating, and it is necessary to combine with other dating methods results to verify the credibility of ESR dating result. By comparing the ESR age (1416 $\pm$ 98 ka) of the T7 lacustrine sediment in Bingcaogang with the burial age of cosmogenic nuclides (1530 $\pm$ 140 ka) of the lacustrine sediment at the same height [26], it was found that the difference between the two is not significant, indicating that the ESR dating results of the sample in this study are relatively reliable. The ESR dating results are shown in Table 1 and in Figures 4 and 6.

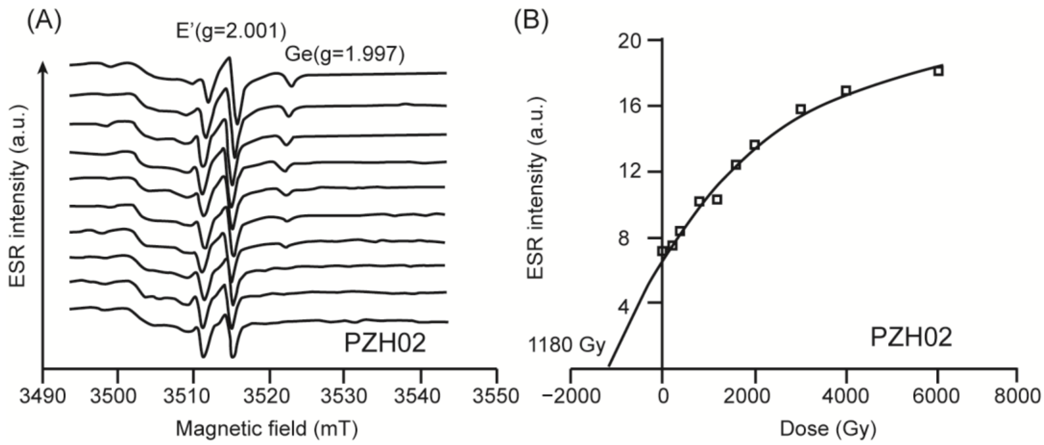

Figure 8. Typical ESR spectrum and additional dose-response curves of a quartz sample. (**A**) ESR spectrum of sample PZH02, showcasing the characteristic signals within the spectrum; (**B**) Additional dose-response curve of sample PZH02, showing the relationship between the received dose and the corresponding ESR signal intensity.

Table 1. ESR sample information and analysis data.

Sample No.	Sampling Site	Altitude (m)	Dating Material	U (μg/g)	Th (μg/g)	K_2O (%)	Water Content (%)	Equivalent Dose (Gy/ka)	Paleodose (Gy)	Age (ka)
PZH01	T7 at Bingcaogang	1335	Lacustrine sediment	1.35	9.20	1.62	2.80	2.65	3751 ± 260	1416 ± 98
PZH02	T1 at Bingcaogang	1047	Fluvial sand	1.42	6.33	1.56	8.25	2.27	1188 ± 208	523 ± 92
PZH03	T5 at Sanduizi	1435	Lacustrine sediment	1.76	12.9	2.34	9.34	3.39	6035 ± 231	1780 ± 68
PZH04	T1 at Sanduizi	1075	Fluvial sand	1.46	9.85	2.23	8.87	3.05	3673 ± 551	1204 ± 181
PZH05	Wanzitou	1208	Lacustrine sediment	1.61	13.7	1.94	9.00	3.09	3175 ± 349	1028 ± 113
PZH06	T3 at Guanyinyan	1140	Fluvial sand	1.87	13.6	2.10	12.56	3.13	2881 ± 331	921 ± 106

The OSL decay curves for sample SHG, as illustrated in Figure 9A, exhibit a rapid decrease in the OSL signals within the first second of stimulation, indicating the dominance of the fast component in the OSL signal. The recuperation of the signal in the absence of dose is found to be below 5% for all samples. Additionally, the recycling ratios for all aliquots fall within the acceptable range of 0.9–1.1. Figure 8B displays the growth curves of four individual aliquots and the Single Grain Characteristics (SGC) curve for sample SHG. None of the four growth curves reach saturation up to a dose of 48 Gy and can be accurately fitted using an exponential plus linear function. The OSL dating results are presented in Table 2 and are also depicted in Figures 3 and 6.

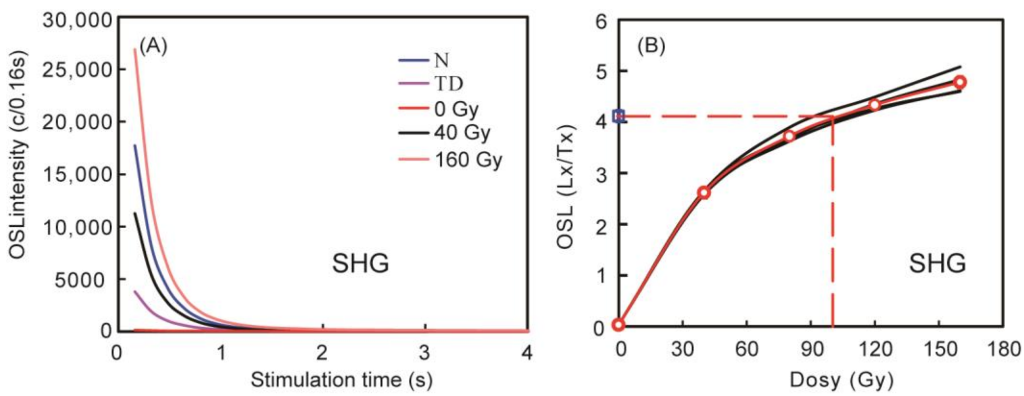

Figure 9. (**A**) The typical OSL shine-down curves of quartz grains, including the natural signal (N), test signal (TD), and regenerate signals at 0 Gy, 48 Gy, and 160 Gy. (**B**) The growth curves of quartz grains. N is natural signal, TD is test signal, 0 Gy, 48 Gy, and 160 Gy are regenerate signals along with the average growth curve represented by a heavier line with empty circles.

Table 2. OSL sample information and analysis data.

Sample No.	Sampling Site	Altitude (m)	Dating Material	K (%)	Th (ppm)	U (ppm)	Water Content (%)	Dose Rate (Gy/ka)	De (Gy)	Age (ka)
SHG	T1 at SHG	1850	Lacustrine sediment	1.94 ± 0.05	15.20 ± 0.40	2.79 ± 0.10	10 ± 5	3.50 ± 0.23	108.57 ± 3.09	31 ± 2.2
LZ	T1 at Lazha	1025	Lacustrine sediment	1.80 ± 0.05	12.6 ± 0.34	3.29 ± 0.11	8 ± 5	3.32 ± 0.22	84.00 ± 4.54	25.3 ± 2.2
TY	T3 at Taoyuan	1298	Lacustrine sediment	1.56 ± 0.05	14.2 ± 0.37	2.54 ± 0.10	10 ± 5	2.91 ± 0.20	225.63 ± 7.32	77.5 ± 5.8

5. Discussion

5.1. The Genesis of the Lacustrine Sediments: Regional Paleo Xigeda Lake or Local Damming Lake

The deposition of lacustrine sediments within the Lower Jinsha River and its primary tributaries plays a critical role in unraveling the historical evolution of drainage patterns in the southeastern Tibetan Plateau. However, the interpretation of these sediments remains a subject of controversy, with two contrasting perspectives in contention. One perspective posits that the lacustrine sediments originated from a vast paleo-lake known as "Xigeda", located in the southeastern Tibetan Plateau [26–28,55]. In contrast, an alternative stance suggests that the lacustrine sediments may have resulted from localized damming of the Jinsha River or its tributaries, highlighting the absence of continuous lacustrine sediments and the presence of landslide deposits as supporting evidence [29–32]. Further investigation and evaluation are crucial to reconcile these differing theories and gain comprehensive insights into the long-term drainage evolution of the southeastern Tibetan Plateau.

Different sedimentary environments can lead to different sedimentary characteristics. If the lacustrine sediments were deposited by a regional paleo-lake, the spatial distribution of lacustrine sediments would be continuous along the river valleys, and the top elevation of lacustrine sediments would be consistent without being uplifted by later differential tectonic uplift. Their deposition age must be consistent or approximate, and the age of the lacustrine sediments should follow the stratigraphic sequence law, namely the younger sediment must be deposited above the older one in one location. If the lacustrine sediments were the result of local landslide-dammed lakes, they should closely trace the river channels in space, and generally present with different deposition ages in different river reaches. In addition, due to river incision, the lacustrine sediments deposited on the upper valley would be generally older than that on the lower valley. Below, we will determine the genesis of the lacustrine sediments based on the spatial distribution, sedimentary characteristics, and sedimentary age of lacustrine sediments combined with the analysis of valley morphology characteristics.

From the spatial distribution of lacustrine sedimentation, the lacustrine sediments are distributed along the trunk and tributaries of the Jinsha River. This is a common phenomenon for dammed lake sediments because they are deposited only after the valley system formation. This phenomenon can be found in other rivers elsewhere, e.g., in the Indus River, numerous stacks of dammed lake sediments have been found to straddle the Indus River and its tributaries and share a distinct horizontal alignment [56]. In the Spiti River, massive relict lacustrine sediments caused by landslide damming were also found to be distributed along the trunk and tributaries [57]. However, the spatial distribution of lacustrine sediments along the river channel is discontinuous and presents a beaded distribution in the plane. Second, there is a significant difference in the altitude of lacustrine sediments in different reaches. Lacustrine sediments in the reaches of Shigu, Taoyuan, Panzhihua, Longjie, and Qiaojia are distributed blow 1800 m, 1670, 1500 m, 1600 m, 1000 m, and 860 m, respectively [17,58,59]. The altitude of the lacustrine sediments shows a gradual downward trend from the upstream to the downstream of the Jinsha River. Therefore, the spatial distribution of lacustrine sediments is closely related to the river channels, indicating that the lacustrine sediments are deposited with the river incision and valley formation, which is inconsistent with the sedimentary characteristics of ancient regional lakes.

From the relationship between lacustrine sediments and other strata, the lacustrine sediments and fluvial gravels are stacked on each other. That is, the lacustrine sediments overlie fluvial gravels, which are also covered by fluvial gravels. In addition, there are also fluvial gravels lenses mixed into the lacustrine sediments, indicating that lacustrine sediments were deposited on fluvial terraces or valley slopes after the formation of river valleys and during or after the deposition process of lacustrine sediment, suggesting that the lacustrine sediments were repeatedly affected by rivers. In the Panzhihua area, lacustrine sediments are not integrated over the underlying ancient strata and ancient soil. In the absence of Neogene strata in the area, a thick layer of late Neogene sedimentation has suddenly accumulated, indicating that the formation process of the lacustrine sediments is very rapid, and that it is unlikely that it was formed by the valley barrier caused by tectonic deformation.

From the deposition age of lacustrine sediment, the deposition age of lacustrine sediments in different river reaches is inconsistent. In the Shigu reach, the deposition age of lacustrine sediments was dated to be 32 ± 2 ka in this study or 20–0.4 ka by Wang et al. (2020) [60]. In the Fengjie reach, the deposition age of lacustrine sediments was dated to be 440–556 ka [59]. In the Taoyuan reach, the deposition age of lacustrine sediments of T3 was dated to be 639 ± 86 ka in this study, or 110~93 ka by Zhu et al. (2019) [61]. In the Panzhihua reach, the deposition age of the lacustrine sediments was dated to be 1780 ± 68 k to 25.3 ± 2.2 ka. In the Longjie reach, the deposition age of lacustrine sediments was dated to be 12.1–7.5 ka [62]. In the Qiaojia reach, the deposition age of lacustrine sediments was dated to be 629–20 ka [17]. Additionally, the lacustrine sediments in the Da River and the Anning River were dated to be 1000–500 ka [32]. Second, in the same river reach, the deposition age of lacustrine terraces with higher altitudes is older than that of lacustrine terraces at low altitudes. In the Panzhihua reach, lacustrine sediments at Wanzitou were dated and yielded an age of 1028 ± 113 ka. Fluvial gravels overlying the lacustrine sediments of T3 at Guanyinyan were dated to be 921 ± 106 ka, suggesting that the lacustrine sediment has been deposited before 921 ± 106 ka. At Bingcaogang, lacustrine sediments of T7 was dated to be 1416 ± 98 ka, and one sample from the fluvial gravels under the lacustrine sediments of T1 yielded an age of 523 ± 92 ka, suggesting that the lacustrine sediments were deposited late than 523 ka. On the Sanduizi profile, a sample of the lacustrine sediments of T5 was measured and yielded an age of 1780 ± 68 ka; fluvial gravels in lacustrine sediments of T1 was dated to be 1204 ± 181 ka. Obviously, the deposition age of lacustrine sediments do not conform to the sedimentary characteristics of a regional paleo-lake.

Therefore, we believe that the lacustrine sediments were not deposited by a regionally giant paleo-lake, namely the "Paleo-lake Xigeda" between the Pliocene to early Pleistocene, but were rather more likely to have been locally deposited by individual dams of landslide, debris flow, and glaciation. Figure 10A shows five ancient damming lakes, but this does not mean that there were only five damming lakes in the Lower Jinsha River. The landslide, debris, and river blocking events are especially prevalent in the Pleistocene around the margins of the Tibetan Plateau due to the strong tectonic activities, high relief, narrow river gorges, and threshold hillslopes [62–68]. Although most dammed lakes will collapse within a few days, there are also dammed lakes that can exist stably for tens of thousands of years, resulting in the accumulation of a large amount of lacustrine sediments in the upstream reach of the damming body [41]. Previous studies have also reported that there are many paleo damming events caused by landslides, mudslides, or glaciers in the Jinsha River valley. For example, the Baimakou landslide may have blocked the Jinsha River and caused the accumulation of lacustrine sediments in the Longjie reach [62]. The Zhaizicun landslide may have blocked the Jinsha River and caused the accumulation of lacustrine sediments in the Taoyuan reach [63]. In the Suwalong section of the Upper Jinsha River, the landslide also blocked the Jinsha River and accumulated a large amount of lacustrine deposits [65,69]. On 10 October and 3 November 2018, two successive landslides occurred at Baige village, which totally dammed the Jinsha River on both occasions, resulting in a dammed lake with a theoretical maximum storage capacity of 7.9×10^8 m^3 [70]. As such, we speculate that many ancient dammed lakes developed in the lower reaches of the Jinsha River, and even the lacustrine sediments in the same reach may have been deposited separately from multiple ancient dammed lakes during the same period. However, due to the lack of chronological data and the insufficient accuracy of dating methods, it is impossible to distinguish the sediments of each dammed lake.

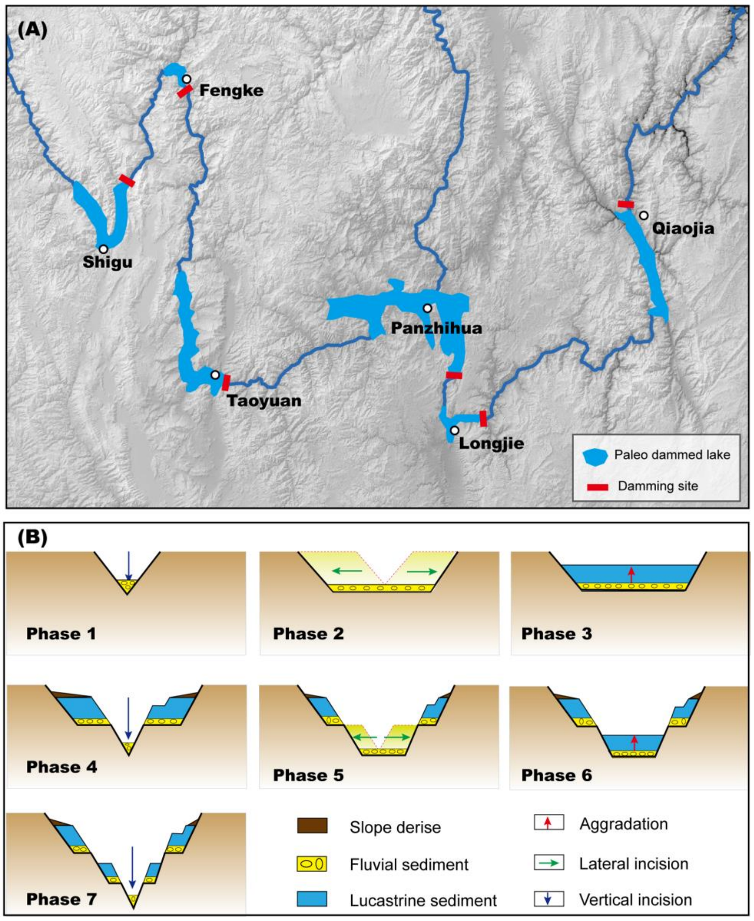

Figure 10. (**A**) Schematic diagram of paleo-dammed lake for deposition of the lacustrine sediments in the Lower Jinsha River. (**B**) The patterns of valley formation of the Lower Jinsha River.

Diachronic lacustrine terraces formed by the dammed lake were widely distributed at different heights in the same reach, indicating that the river has been repeatedly blocked in the downstream gorges, leading to aggradation in the upstream reaches. When the lake was filled or a landslide dam was cut through, the river would incise upstream, and the channel would cut down again from the lacustrine sediments, sometimes accompanied by the development of a series of cut-in-fill terraces on the lacustrine sediments. With the river incision, the height of the riverbed gradually decreases, vertical incision combined with lateral incision will make the valley steep enough, and then a landslide happens again, blocking the river and impounding a lake to deposit lacustrine sediments at a lower height of the river valley. These processes happened one after another as the river incised down. Therefore, the valley development of the Jinsha River was mainly occupied by the major episodes of aggradation and incision. The continuity of the river process is shown as "incision-landslide-damming-aggradation-incision", while the interval in this process still leads to the development of terrace sequences (Figure 10B).

5.2. Incision Time of the Lower Jinsha River

The viewpoints on the formation time of the Jinsha River valley have yet to reach a consensus, spanning from the Paleocene to the Pleistocene [14,16–18,21,28,71].

Planation surfaces, which were regarded as the starting point of the birth of river valley systems [72], are widely distributed in the southeastern Tibetan Plateau, with an age of Pliocene to Early Pleistocene [36,73], indicating that the paleo-drainage system in the formation period of the planation surface has been reorganized in the early Pleistocene. The modern valley systems of the Jinsha River were incised by themselves from the planation surfaces, with no or only little relationship with the paleo-drainage system. Therefore, the modern Jinsha River valley formed after the disintegration of planation surfaces induced by the surface uplift of the Yunnan Plateau since the Pliocene.

The formation of landslide-dammed lakes requires the river valley to be cut down to a certain depth, so the dammed lake deposits and the lacustrine terraces are the signs of the valley cutting down. The dammed lake sediments have been appeared in the Panzhihua reach at least 1.78 Ma ago, indicating that the Jinsha River has incised its valley prior to 1.78 Ma. Many previous studies of river terraces and associated sediments in other reaches of the Jinsha River support this conclusion. For example, fluvial terraces immediately upstream of the Shigu were developed around 1.54 Ma, and river terraces from Shigu to Yibin were formed around 1.78 Ma B.P. [55]; Fluvial terraces near the Jinjiangjie were dated to 1.02 Ma [74]. The fluvial terrace near Qiaojia was formed at about 1.2 Ma [17,73]. The high-level river terraces from Yongshan to Yibin were formed between 1.17~1.02 Ma [11]. River terraces in the lower Yalong River, which is a tributary of the Jinsha River, also formed around 1.1 Ma [75]. This evidence from the valley landforms and sediments demonstrated that the valley system of the modern Jinsha River was formed in the late Early Pleistocene (Figure 11).

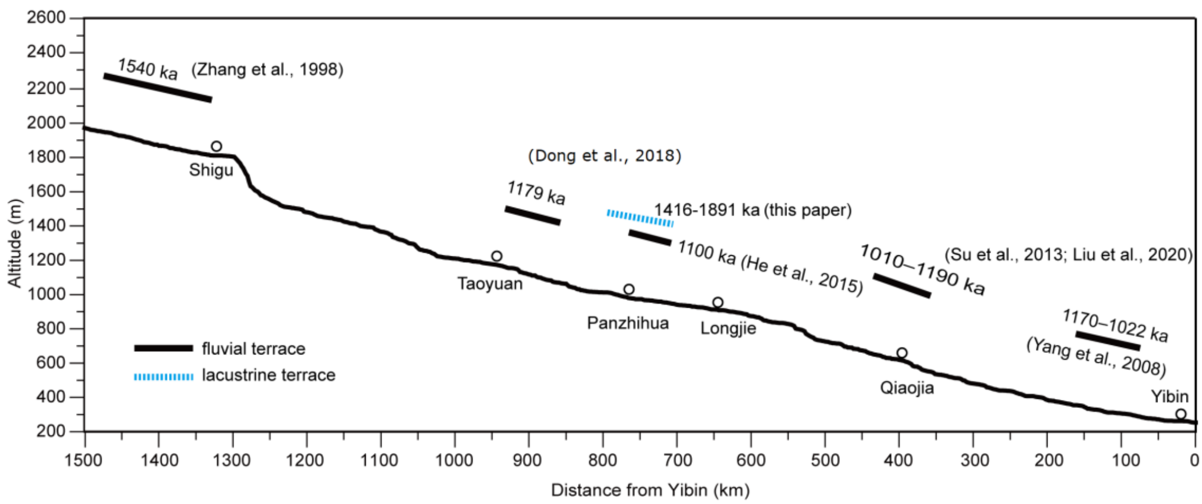

Figure 11. The high terraces with ages along the Lower Jinsha River [11,17,55,73–75].

6. Conclusions

Through sedimentological analysis and chronological determination of the fluvio-lacustrine sediments of the lower Jinsha River, we found that lacustrine sediment in this reach is discontinuous in spatial distribution but is closely distributed along the main and tributary channel. The lacustrine sediments are stacked with fluvial sand and gravels, and are in unconformable contact with the underlying bedrock strata or weathered crust. The elevation and deposition age of lacustrine sediments are significant different in different reaches. The lacustrine sediments in same reach are distributed in a stepped pattern on the valley profile, and the sedimentation age of high-altitude fluvial terraces is earlier than that of low-altitude fluvial terraces. The oldest lacustrine terrace here were dated to be 1.78 Ma. We suggest that the lacustrine sediments were deposited by individual local dammed lakes. The modern Jinsha River began to incise its valley before the Early Pleistocene.

Author Contributions: H.G. designed the experiments. Z.L. and F.L. performed the experiments. All authors analyzed the data. F.L. wrote the manuscript with help from the other authors. All authors have read and agreed to the published version of the manuscript.

Funding: This work was financially supported by the National Science Foundation of China (grant no. 42101005), the Hunan Provincial Natural Science Foundation of China (grant no. 2021JJ40023), the Outstanding Youth Project of Hunan Department of Education (grant no. 20B106), and the Research Foundation of the Department of Natural Resources of Hunan Province (grant no. 20230135DZ).

Data Availability Statement: Not applicable.

Acknowledgments: We thank Huai Su for fielding works, Fuqiang Li and Dianbao Chen for assisting with sampling.

Conflicts of Interest: The authors declare no conflict of interest.

References

1. Potter, P.E. Significance and origin of big rivers. *J. Geol.* **1978**, *86*, 13–33. [CrossRef]
2. Ward, F.K. The hydrography of the Yunnan-Tibet frontier. *Geogr. J.* **1918**, *52*, 288–299. [CrossRef]
3. Davis, W.M. Drainage Evolution on the Yünnan-Tibet Frontier. *Geogr. Rev.* **1919**, *7*, 413–415. [CrossRef]
4. Lee, C.Y. The development of the upper Yangtze valley. *Bull. Geol. Soc. China* **1934**, *13*, 107–118. (In Chinese) [CrossRef]
5. Barbour, G.B. Physiographic history of the Yangtze. *Geogr. J.* **1936**, *87*, 17–32. [CrossRef]
6. Li, C.S. Development history of the Yangtze River. *Yangtze River* **1956**, *12*, 3–6. (In Chinese)
7. Yuan, F.L. Supplementay study on the development history of the Yangtze River. *J. People's Yangtze River* **1957**, *2*, 1–9. (In Chinese)
8. Ren, M.E.; Bao, H.S.; Han, T.C.; Wang, F.Y.; Huang, P.H. The problems of valley landforms and river capture of the Jinshajiang River in northwestern Yunnan. *Acta Geogr. Sin.* **1959**, *25*, 135–155.
9. He, H.S.; He, K.Z.; Zhu, X.M.; Zhu, Z.Y. A discussion on the problem of river-capture of the Jinshajiang River in Northwest Yunnan. *Geoscience* **1989**, *3*, 319–330. (In Chinese)
10. Chen, J. Discussion on the evolutionary history of Jinsha River from Benzilan to Jinjiangjie in northwestern Yunnan. *J. East China Geol. Inst.* **1994**, *17*, 234–253. (In Chinese)
11. Yang, D.Y.; Han, Z.Y.; Ge, Z.S. Geomorphic processs of the formation and incision of the section from Shigu to Yibin of the Jinshajiang River. *Quat. Sci.* **2008**, *28*, 564–568. (In Chinese)
12. Ouimet, W.; Whipple, K.; Royden, L.; Reiners, P.; Hodges, K.; Pringle, M. Regional incision of the eastern margin of the Tibetan Plateau. *Lithosphere* **2010**, *2*, 50–63. [CrossRef]
13. Zheng, H.B.; Clift, P.D.; Wang, P.; Tada, R.; Jia, J.T.; He, M.Y.; Jourdan, F. Pre-Miocene birth of the Yangtze River. *Proc. Natl. Acad. Sci. USA* **2013**, *110*, 7556–7561. [CrossRef] [PubMed]
14. McPhillips, D.; Hoke, G.D.; Liu-Zeng, J.; Bierman, P.R.; Rood, D.H.; Niedermann, S. Dating the incision of the Yangtze River gorge at the First Bend using three-nuclide burial ages. *Geophys. Res. Lett.* **2016**, *43*, 101–110. [CrossRef]
15. Shen, X.; Tian, Y.; Li, D.; Li, D.; Qin, S.; Pieter, V.; James, S. Oligocene-Early Miocene river incision near the first bend of the Yangze River: Insights from apatite (U-Th-Sm)/He thermochronology. *Tectonophysics* **2016**, *687*, 223–231. [CrossRef]
16. Su, H.; Dong, M.; Hu, Z.B. Late Miocene birth of the Middle Jinsha River revealed by the fluvial incision rate. *Glob. Planet. Change* **2019**, *183*, 103002. [CrossRef]
17. Liu, F.L.; Gao, H.S.; Li, Z.M.; Pan, B.T.; Su, H. Terraces development and their implications for valley evolution of the Jinsha River from Qiaojia to Menggu. *Acta Geogr. Sin.* **2020**, *75*, 1095–1105.
18. Zheng, H.; Clift, P.D.; He, M.; Bian, Z.; Liu, G.; Liu, X.; Xia, L.; Yang, Q.; Jourdan, F. Formation of the First Bend in the late Eocene gave birth to the modern Yangtze River, China. *Geology* **2021**, *49*, 35–39. [CrossRef]
19. Zhang, Z.; Daly, J.S.; Tian, Y.; Wang, Y.; Eszter, B.; Sun, X.; Liu, Y. Sedimentary recycling in Jianchuan Basin, SE Tibet: A solution to the debate on the formation age of the First Bend (Yangtze River). *Geomorphology* **2023**, *440*, 108888. [CrossRef]
20. Rohrmann, A.; Kirby, E.; Schwanghart, W. Accelerated Miocene incision along the Yangtze River driven by headward drainage basin expansion. *Sci. Adv.* **2023**, *9*, eadh1636. [CrossRef]
21. Clark, M.K.; House, M.A.; Royden, L.H.; Whipple, K.X.; Burchfiel, B.C.; Zhang, X.; Tang, W. Late Cenozoic uplift of southeastern Tibet. *Geology* **2005**, *33*, 525–528. [CrossRef]
22. Clift, P.D.; Blusztajn, J.; Nguyen, A.D. Large-scale drainage capture and surface uplift in eastern Tibet-SW China before 24 Ma inferred from sediments of the Hanoi Basin, Vietnam. *Geophys. Res. Lett.* **2006**, *33*, L19403. [CrossRef]
23. Zhao, M.; Shao, L.; Liang, J.; Li, Q. No Red River capture since the late Oligocene: Geochemical evidence from the northwestern South China Sea. *Deep. Sea Res. Part II Top. Stud. Oceanogr.* **2015**, *122*, 185–194. [CrossRef]
24. Wei, H.H.; Wang, E.; Wu, G.L.; Meng, K. No sedimentary records indicating southerly flow of the paleo upperYangtze River from the first bend in southeastern Tibet. *Gondwana Res.* **2016**, *32*, 93–104. [CrossRef]
25. Wissink, G.K.; Hoke, G.D.; Garzione, C.N.; Liu-Zeng, J. Temporal and spatial patterns of sediment routing across the southeast margin of the Tibetan Plateau: Insights from detrital zircon. *Tectonics* **2016**, *35*, 2538–2563. [CrossRef]

26. Kong, P.; Granger, D.E.; Wu, F.Y.; Caffee, M.W.; Wang, Y.J.; Zhao, X.T.; Zheng, Y. Cosmogenic nuclide burial ages and provenance of the Xigeda paleo-lake: Implications for evolution of the Middle Yangtze River. *Earth Planet. Sci. Lett.* **2009**, *278*, 131–141. [CrossRef]
27. Deng, B.; Chew, D.; Mark, C.; Liu, S.G.; Cogné, N.; Jiang, L.; O'Sullivan, G.; Li, Z.W.; Li, J.X. Late Cenozoic drainage reorganization of the paleo-Yangtze river constrained by multi-proxy provenance analysis of the Paleo-lake Xigeda. *GSA Bull.* **2021**, *133*, 199–211. [CrossRef]
28. Zhao, X.; Zhang, H.; Tao, Y.; Wang, Y.; Pang, J.; Ma, Y.; Zhang, J.; Ma, Z.; Xiong, J. Pliocene to Early Pleistocene drainage reorganization in eastern Tibet inferred from detrital zircons. *Geophys. Res. Lett.* **2021**, *48*, e2021GL094563. [CrossRef]
29. Chen, Z.L.; Sun, Z.P.; Royden, L.H.; Zhang, X.Y. Landslide blocked lake: Origin of the Xigeda Formation in Luding, Sichuan and its significance. *Quat. Sci.* **2014**, *24*, 614–620. (In Chinese)
30. Wang, P.; Li, J.P.; Wang, J.C.; Liu, C.R.; Han, F.; Gao, L. Quartz Ti-center in ESR dating of Xigeda formation in Sichuan and contrast with magnetic stratigraphic profiles. *Nucl. Tech.* **2011**, *34*, 111–115. (In Chinese)
31. Xu, Z.M.; Liu, W.L. Some problems in the study of the genesis of Xigeda Formation. *Earth Sci. Front.* **2011**, *18*, 256–270. (In Chinese)
32. Yang, Y.; Xu, S.; Binnie, S.A.; Ritter, B.; Cui, L.F.; Cao, Z.P.; Zhang, S.C.; Liu, C.Q.; Dunai, T. Late Cenozoic locally landslide-dammed lakes across the Middle Yangtze River. *Geomorphology* **2022**, *413*, 108366. [CrossRef]
33. Gopinath, G.; Resmi, T.R.; Karunakara, N.; Manjula, P.; Jesiya, N.P.; Kumara, K.S.; Srinivas, R. How Long a Tropical Mountainous Lake Can Survive? Inferences from Geochemistry and Radiometric Measurements of Pookode Lake, Kerala, India. *J. Geol. Soc. India* **2023**, *99*, 840–846. [CrossRef]
34. Giano, S.I.; Schiattarella, M. Drainage integration of small endorheic basins at the Pleistocene-Holocene transition: An example from southern Italy. *Geomorphology* **2023**, *427*, 108622. [CrossRef]
35. Clark, M.K.; Royden, L.H.; Whipple, K.X.; Burchfiel, B.C.; Zhang, X.; Tang, W. Use of a regional, relict landscape to measure vertical deformation of the eastern Tibetan Plateau. *J. Geophys. Res. Earth Surf.* **2006**, *111*, F03002. [CrossRef]
36. Liu, F.L.; Gao, H.S.; Pan, B.T.; Li, Z.M.; Su, H. Quantitative analysis of planation surfaces of the upper Yangtze River in the Sichuan-Yunnan Region, Southwest China. *Front. Earth Sci.* **2019**, *13*, 55–74. [CrossRef]
37. Burchfiel, B.C.; Chen, Z.L.; Liu, Y.P.; Royden, L.H. Tectonics of the Longmen Shan and adjacent regions, central China. *Int. Geol. Rev.* **1995**, *37*, 661–735. [CrossRef]
38. Wang, E.; Kirby, E.; Furlong, K.P.; Soest, M.v.; Xu, G.; Shi, X.; Kamp, P.J.J.; Hodges, K.V. Two-phase growth of high topography in eastern Tibet during the Cenozoic. *Nat. Geosci.* **2012**, *5*, 640–645. [CrossRef]
39. Sichuan Bureau of Geology and Mineral Resources (SBGMR). *Regional Geology of Sichuan Province*; Geological Publishing House: Beijing, Chian, 1991.
40. Burchfiel, B.C.; Chen, Z. (Eds.) Tectonics of the Southeastern Tibetan Plateau and Its Adjacent Foreland. Geological Society of America: Boulder, CO, USA, 2012.
41. Costa, J.E.; Schuster, R.L. The formation and failure of natural dams. *Geol. Soc. Am. Bull.* **1998**, *100*, 1054–1068. [CrossRef]
42. Fan, X.M.; Dufresne, A.; Subramanian, S.S.; Strom, A.; Hermanns, R.; Stefanelli, C.T.; Hewitt, K.; Yunus, A.P.; Dunning, S.; Capra, L.; et al. The formation and impact of landslide dams-state of the art. *Earth Sci. Rev.* **2020**, *203*, 103116. [CrossRef]
43. Liu, C.R.; Yin, G.M.; Gao, L.; Bahain, J.J.; Li, J.P.; Lin, M.; Chen, S.M. ESR dating of Pleistocene archaeological localities of the Nihewan Basin, North China-Preliminary results. *Quat. Geochronol.* **2010**, *5*, 385–390. [CrossRef]
44. Rixhon, G.; Briant, R.M.; Cordier, S.; Duval, M.; Jones, A.; Scholz, D. Revealing the pace of river landscape evolution during the Quaternary: Recent developments in numerical dating methods. *Quat. Sci. Rev.* **2017**, *166*, 91–113. [CrossRef]
45. Duval, M.; Arnold, L.J.; Rixhon, G. Electron spin resonance(ESR) dating in Quaternary studies: Evolution, recent advances and applications. *Quat. Int.* **2020**, *556*, 1–10. [CrossRef]
46. Del, V.M.; Alonso, M.J.; Duval, M.; Arriolabengoa, M.; Álvarez, I.; Bodego, A.; Cheng, H.; Hermoso de Mendoza, A.; Aranburu, A.; Iriarte, E. Luminescence and ESR dating of thesedimentary infill from the multi-level cave system of Alkerdi-Zelaieta(Navarre, N Spain). *Quat. Geochronol.* **2022**, *73*, 101380. [CrossRef]
47. Yokoyama, Y.; Falgueres, C.; Quaegebeur, J.P. ESR dating of quartz from Quaternary sediments: First attempt. *Nucl. Tracks Radiat. Meas. (1982)* **1985**, *10*, 921–928. [CrossRef]
48. Lai, Z.P. Testing the use of an OSL standardised growth curve (SGC) for De determination on quartz from the Chinese Loess Plateau. *Radiat. Meas.* **2006**, *41*, 9–16. [CrossRef]
49. Murray, A.S.; Wintle, A.G. Luminescence dating of quartz using an improved single-aliquot regenerative-dose protocol. *Radiat. Meas.* **2000**, *32*, 57–73. [CrossRef]
50. Roberts, H.M.; Duller, G.A.T. Standardised growth curves for optical dating of sediment using multiple-grain aliquots. *Radiat. Meas.* **2004**, *38*, 241–252. [CrossRef]
51. Aitken, M.J. *Thermoluminescence Dating*; Academic Press: London, UK, 1985.
52. Zhao, X.T.; Wu, Z.H.; Feng, Y.Y.; Zhang, Y.S.; Hu, D.G.; Qu, Y.X.; Guo, C.B. Landscapes and sediments ofthe'Yangtze First Bend'valley along the Jinsha River and development of the valley. *Geol. Bull. China* **2015**, *34*, 83–103.
53. Xu, Z.M. Deposits of Zhaizicun Landslide-dammed lake along Jinsha River and its implication for the genesis of Xigeda Formation. *Geol. Rev.* **2011**, *57*, 675–686. (In Chinese)

54. Zhao, X.T.; Hu, D.G.; Zhang, Y.S. Genesis and age of the gravels underlying the Xigeda Formation of Panzhihua, Sichuan, China, and valley development of the ancient Jinsha River. *Acta Geosci. Sin.* **2008**, *29*, 1–12. (In Chinese)
55. Zhang, Y.C.; Li, J.J.; Zhu, J.J.; Chen, Y.; Pan, B.T.; Kuang, M.S. Studies on development of Jinshajiang River during Late Cenozoic. *Yunnan Geogr. Environ. Res.* **1998**, *10*, 43–48. (In Chinese)
56. Blöthe, J.H.; Munack, H.; Korup, O.; Fülling, A.; Garzanti, E.; Resentini, A.; Kubik, P.W. Late Quaternary valley infill and dissection in the Indus River, western Tibetan Plateau margin. *Quat. Sci. Rev.* **2014**, *94*, 102–119. [CrossRef]
57. Phartiyal, B.; Anupam, S.; Pradeep, S.; Yogesh, R. Chronology of relict lake deposits in the Spiti River, NW Trans Himalaya: Implications to Late Pleistocene-Holocene climate-tectonic perturbations. *Geomorphology* **2009**, *108*, 264–272. [CrossRef]
58. Liu, F.L.; Gao, H.S.; Li, Z.M.; Pan, B.T.; Su, H. Terraces development and their implications for valley evolution of the Jinsha River since Late Pleistocene near Longjie, Yunnan. *Adv. Earth Sci.* **2020**, *35*, 431. (In Chinese)
59. Wang, K.; Yin, G.M.; Wei, C.Y.; Chen, L.; Liu, C.R.; Wang, W.B. ESR chronology of lacustrine sediment in the Fengke reaches of the middle Jinsha River: Implications for landslide dammed lake formation. *J. Earth Environ.* **2022**, *13*, 270–280. (In Chinese)
60. Wang, H.; Tong, K.; Hu, G.; Wang, P.; Li, D.H.; Huang, J.W.; Cao, G.R.; Zhang, J.F.; Chen, J. Dam and megafloods at the First Bend of the Yangtze River since the Last Glacial Maximum. *Geomorphology* **2021**, *373*, 107491. [CrossRef]
61. Zhu, Z.F.; Su, H.; Dong, M.; Ming, Q.Z.; Shi, Z.T. The age of Zhaizicun ancient dammed lake sediments in Jinsha River. *Quat. Sci.* **2018**, *38*, 145–150. (In Chinese)
62. Liu, W.M.; Hu, K.H.; Carling, P.A.; Carling, P.A.; Lai, Z.P.; Cheng, T.; Xu, Y.L. The establishment and influence of Baimakou paleo-dam in an upstream reach of the Yangtze River, southeastern margin of the Tibetan Plateau. *Geomorphology* **2018**, *321*, 167–173. [CrossRef]
63. Chai, H.J.; Liu, H.C.; Zhang, Z.Y. The catalog of Chinese landslide dam events. *J. Geol. Hazards Environ. Preserv.* **1995**, *6*, 1–9. (In Chinese)
64. Zhang, Y.S.; Zhao, X.T.; Lan, H.X.; Xiong, T.Y. A Pleistocene landslide-dammed lake, Jinsha River, Yunnan, China. *Quat. Int.* **2011**, *233*, 72–80. [CrossRef]
65. Chen, J.; Dai, F.; Lv, T.; Cui, Z. Holocene landslide-dammed lake deposits in the Upper Jinsha River, SE Tibetan Plateau and their ages. *Quat. Int.* **2013**, *298*, 107–113. [CrossRef]
66. Higgitt, D.L.; Zhang, X.B.; Liu, W.M.; Tang, Q.; He, X.B.; Ferrant, S. Giant palaeo-landslide dammed the Yangtze river. *Geosci. Lett.* **2014**, *1*, 6. [CrossRef]
67. Bao, Y.D.; Zhai, S.J.; Chen, J.P.; Xu, P.H.; Sun, X.H.; Zhan, J.W.; Zhang, W.; Zhou, X. The evolution of the Samaoding paleolandslide river blocking event at the upstream reaches of the Jinsha River, Tibetan Plateau. *Geomorphology* **2020**, *351*, 106970. [CrossRef]
68. Fan, X.M.; Xu, Q.; Alonso-Rodriguez, A.; Subramanian, S.S.; Li, W.L.; Zheng, G.; Dong, X.J.; Huang, R.Q. Successive landsliding and damming of the Jinsha River in eastern Tibet, China: Prime investigation, early warning, and emergency response. *Landslides* **2019**, *16*, 1003–1020. [CrossRef]
69. Li, Y.; Chen, J.P.; Zhou, F.J.; Song, S.Y.; Zhang, Y.W.; Gu, F.F.; Chen, C. Identification of ancient river-blocking events and analysis of the mechanisms for the formation of landslide dams in the Suwalong section of the upper Jinsha River, SE Tibetan Plateau. *Geomorphology* **2020**, *368*, 107351. [CrossRef]
70. Zhong, Q.; Chen, S.; Wang, L.; Shan, L. Back analysis of breaching process of Baige landslide dam. *Landslides* **2020**, *17*, 1681–1692. [CrossRef]
71. Zhang, D.; Cao, K.; Yuan, X.; Wang, G.; Beek, P.v.d. Late Oligocene-early Miocene Origin of the First Bend of the Yangtze River explained by thrusting-induced river reorganization. *Geomorphology* **2022**, *411*, 108303. [CrossRef]
72. Davis, W.M. The geographical cycle. *Geogr. J.* **1899**, *14*, 481–504. [CrossRef]
73. Su, H.; Ming, Q.Z.; Pan, B.T.; Gao, H.S.; Zhang, W.X.; Dong, M.; Shi, Z.T. The analysis and discussions on the chronological frame of Jinshajiang River Vally-drainage. *J. Mt. Sci.* **2013**, *31*, 685–692. (In Chinese)
74. Dong, M.; Su, H.; Shi, Z.T.; Ming, Q.Z.; He, H.L. The age of river terraces in the Jinjiangjie reach of the Jinsha River and its implications for valley and drainage evolution. *Acta Geogr. Sin.* **2018**, *73*, 1728–1736. (In Chinese)
75. He, Z.; Zhang, X.; Bao, S.; Qiao, Y.S.; Sheng, Y.Y.; Liu, X.T.; He, X.T.; Yang, X.C.; Zhao, J.X.; Liu, R. Multiple climatic cycles imprinted on regional uplift-controlled fluvial terraces in the lower Yalong River and Anning River, SE Tibetan Plateau. *Geomorphology* **2015**, *250*, 95–112. [CrossRef]